Ferristatin II Promotes Degradation of Transferrin Receptor-1 In Vitro and In Vivo

OPEN ACCESS Freely available online

PLOS ONE

Ferristatin II Promotes Degradation of Transferrin Receptor-1 *In Vitro* and *In Vivo*

Shaina L. Byrne[1☯], Peter D. Buckett[1☯], Jonghan Kim[1], Flora Luo[1], Jack Sanford[1], Juxing Chen[2], Caroline Enns[2], Marianne Wessling-Resnick[1]*

1 Department of Genetics and Complex Diseases, Harvard School of Public Health, Boston, Massachusetts, United States of America, **2** Department of Cell Biology, Oregon Health Sciences Center, Portland, Oregon, United States of America

Abstract

Previous studies have shown that the small molecule iron transport inhibitor ferristatin (NSC30611) acts by down-regulating transferrin receptor-1 (TfR1) via receptor degradation. In this investigation, we show that another small molecule, ferristatin II (NSC8679), acts in a similar manner to degrade the receptor through a nystatin-sensitive lipid raft pathway. Structural domains of the receptor necessary for interactions with the clathrin pathway do not appear to be necessary for ferristatin II induced degradation of TfR1. While TfR1 constitutively traffics through clathrin-mediated endocytosis, with or without ligand, the presence of Tf blocked ferristatin II induced degradation of TfR1. This effect of Tf was lost in a ligand binding receptor mutant G647A TfR1, suggesting that Tf binding to its receptor interferes with the drug's activity. Rats treated with ferristatin II have lower TfR1 in liver. These effects are associated with reduced intestinal ^{59}Fe uptake, lower serum iron and transferrin saturation, but no change in liver non-heme iron stores. The observed hypoferremia promoted by degradation of TfR1 by ferristatin II appears to be due to induced hepcidin gene expression.

Citation: Byrne SL, Buckett PD, Kim J, Luo F, Sanford J, et al. (2013) Ferristatin II Promotes Degradation of Transferrin Receptor-1 *In Vitro* and *In Vivo*. PLoS ONE 8(7): e70199. doi:10.1371/journal.pone.0070199

Editor: Makoto Kanzaki, Tohoku University, Japan

Received May 6, 2013; **Accepted** June 14, 2013; **Published** July 23, 2013

Funding: The research reported in this publication was supported by the National Institute of Diabetes, Digestive and Kidney Diseases of the National Institutes of Health under award numbers R01DK046750 and RC1DK086744 to MW-R and award number R37DK054488 to CAE. SLB was supported by the National Institute of Environmental Health Sciences of the National Institutes of Health under award number T32ES016645. The funders had no role in study design, data collection and analysis, decision to publish, or preparation of the manuscript.

Competing Interests: The authors have declared that no competing interests exist.

* E-mail: wessling@hsph.harvard.edu

☯ These authors contributed equally to this work.

Introduction

Iron is involved in various processes of cellular homeostasis including DNA synthesis and repair, ATP synthesis, and oxygen transport [1]. It is essential for life and depletion of iron restricts growth of cells [2,3,4]. Iron is absorbed from the diet by duodenal enterocytes and is transported to the periphery bound to transferrin (Tf). At neutral pH, holo-Tf binds to receptors on the cell surface [5]. This complex undergoes clathrin-dependent endocytosis and is delivered to early endosomes [6]. Within the low pH environment of the endosome, iron is released from Tf. Iron is reduced from ferric iron (Fe^{3+}) to ferrous iron (Fe^{2+}) by the ferrireductase Steap3 [7,8]. Ferrous iron is then transported into the cytosol via divalent metal transporter-1 (DMT-1) [9], ZIP14 [10] and/or TRPML [11]. The ligand-receptor complex, devoid of iron, is recycled back to the plasma membrane where apo-Tf dissociates and continues the cycle of iron acquisition and delivery to peripheral tissues [12,13].

There are two known Tf receptors, TfR1 and TfR2. At the cellular level, TfR1 is ubiquitously expressed and is largely responsible for Tf-mediated delivery of iron to peripheral tissues [14]. TfR1 is a constitutively recycling receptor that undergoes clathrin-mediated endocytosis with or without its ligand [12,15]. It is widely held that the presence of TfR1 identifies the endocytic, sorting and recycling compartments of most cells. Often marked by fluorescently labeled Tf or receptor immunoreactivity, TfR1 is frequently used as a reference marker for these domains [16,17]. The interactions of TfR1 with the clathrin machinery also provide a paradigm for how membrane proteins engage with coated pits and become internalized by coated vesicles [18]. In particular, receptor interactions with the clathrin adaptor protein AP-2 have been studied at the molecular and structural level [19,20,21]. At the plasma membrane, interactions with the AP-2 adaptor complex mediate assembly of clathrin triskelions that form a budding coated pit that is pinched off by dynamin to generate a coated vesicle [22,23].

At the systemic level, regulation of iron homeostasis has been elucidated through studies of hereditary hemochromatosis [24]. Mutations in HFE [25], transferrin receptor-2 [26], ferroportin [27], hepcidin [28], or hemojuvelin [29] have been identified in different forms of human disease. Iron metabolism is regulated through a complex network of protein-protein interactions between these factors. Although TfR1 is ubiquitously expressed and plays a key role in iron delivery through receptor-mediated endocytosis of diferric transferrin, HFE and TfR2 play a more specialized role in the liver where they have been shown to act as upstream regulators of hepcidin synthesis [30]. A model has been proposed wherein HFE interactions with TfR1 limit its association with TfR2 [31]. When iron levels increase, saturation of Tf promotes receptor binding, which in turn competitively displaces HFE from TfR1 to allow its interaction with TfR2 [32]. Over-

expression of HFE in the livers of mice increases hepcidin expression, supporting the notion that levels of endogenous protein are limiting [30,33].

Hepcidin, a 25 amino acid peptide hormone, is secreted primarily by the liver and regulates systemic iron status [34]. The peptide binds to the iron exporter ferroportin (Slc40a1), inducing its internalization and lysosomal degradation [35]. This mechanism controls intestinal iron efflux and recycling of iron from macrophages [36,37]. Concordantly, hepcidin synthesis increases with iron loading and decreases with iron deficiency [38,39]. Hepcidin levels are inappropriately low in hemochromatosis patients with mutations in HFE [40] and TfR2 [41].

Genetic approaches to understanding iron homeostasis have been complemented by the recent development of pharmacological tools to either inhibit or activate transport and regulatory factors involved in iron metabolism [42]. One approach to further our understanding of the regulation of iron transport and homeostasis at the molecular level is through the use of small molecule inhibitors. Using a cell-based fluorescence screening strategy, ferristatin (NSC306711) was initially identified as an inhibitor of Tf-mediated iron delivery [43]. Characterization of ferristatin's action revealed that it promoted the degradation of TfR1 in a nystatin-sensitive fashion. Internalization and receptor down-regulation of TfR1 in the presence of ferristatin occurred in a clathrin- and dynamin-independent manner [44]. These results were unexpected given the established role of clathrin-mediated endocytosis in TfR1 membrane trafficking, but were specific to this receptor since ferristatin did not alter LDL receptor trafficking [44]. More recently, NSC8679 (referred to here as ferristatin II) was identified as a polysulphonated dye not only structurally related to ferristatin but with functional similarities as well [45]. This investigation was undertaken to characterize ferristatin II action and the nature of the nystatin-sensitive clathrin-independent mechanism for TfR1 down-regulation. The alternative lipid raft mediated trafficking and degradation pathway revealed by the ferristatins may hold clinical potential to limit iron acquisition. This idea is supported by results of *in vivo* experiments that reveal a systemic effect on iron metabolism upon treatment with ferristatin II.

Materials and Methods

Ethics Statement

This study was performed in strict accordance with the recommendations in the Guide for the Care and Use of Laboratory Animals of the National Institutes of Health. The protocol was approved by the Harvard Medical Area Animal Care and Use Committee (Animal Experimentation Protocol AEP #04692).

Cell Culture

HeLa cells were grown in Dulbecco's minimal essential medium (DMEM) containing 50 U/mL penicillin, 50 μg/mL streptomycin, L-glutamine, and 10% fetal bovine serum (FBS, Sigma). TRVb cells [46] (a kind gift of Dr. Timothy E. McGraw, Weill Medical College, Cornell University) were grown in Ham's F-12 medium containing 10% FBS. Stably transfected TRVb cells containing either WT TfR1, Y20C/F23A TfR1 or Δ3–28 TfR1 were grown in Ham's F-12 containing 5 g/L glucose, 400 μg/mL G418 and 5% FBS. Hep3B cells stably expressing human TfR2 [47] were maintained in minimal essential medium (MEM) containing 1 mM sodium pyruvate, 0.1 mM non-essential amino acids, 10% FBS and 400 μg/mL G418.

Ferristatin II Treatment: *In vitro*

Ferristatin II (NSC8679) was obtained from Sigma (Product No. C1144, also called Chlorazol Black or Direct Black 38). For treatment with ferristatin II, cells were first washed three times with phosphate-buffered saline containing 1 mM $MgCl_2$ and 0.1 mM $CaCl_2$ (PBS^{++}) and then washed once with serum-free medium. Fifty μM ferristatin II or DMSO control was added to cells in serum free medium. To inhibit lysosomal degradation of TfR1, cells were treated overnight with 10 nM Bafilomycin A_1 (Sigma, B1793). To disrupt lipid rafts, cells were pretreated for 20 minutes with 25 μg/mL nystatin (Sigma) before addition of ferristatin II. Cells were incubated at 37°C with 5% CO_2 for 4 hours unless otherwise stated.

Ferristatin II Treatment: *In vivo*

Male Sprague-Dawley rats (3-wk-old) were injected twice daily for 1 or 3 days with ferristatin II (up to maximum of 40 mg/kg) or saline as a vehicle control. On day 2 or day 4, rats were injected once and fasted for 6 hours. At the start of the fasting period, rats were housed in metabolic cages for 6 h to collect urine. For ^{59}Fe tracer studies, on day 4 rats were fasted for 4 h prior to administration of ^{59}Fe by gavage (1 μl/g body weight of a solution of 30 μCi/ml, diluted in 20 mM Tris, 150 mM NaCl, pH 5.7 with 10 mM freshly dissolved ascorbate). Blood samples were taken at intervals from 15 min to 1 h and radioactivity was determined by gamma counting. At the end of the study, rats were euthanized by isoflurane overdose followed by exsanguination for collection of tissues to analyze iron status.

Western Blot Analysis

After incubation with ferristatin II as described above, cells were washed three times with ice cold PBS^{++} and lysed in NET lysis buffer (150 mM NaCl, 5 mM EDTA, 10 mM Tris pH 7.4 and 1% Triton X-100) containing protease inhibitors (Protease Inhibitor Set lll, Calbiochem) for 20 minutes on ice. Lysates were cleared at 16,000×g for 10 minutes at 4°C and 20–60 μg of the supernatant were loaded on 8% SDS-polyacrylamide gels. Livers from rats treated with ferristatin ll or vehicle control were homogenized in RIPA buffer (10 mM Tris, pH 7.4, 150 mM NaCl, 1.0 mM EDTA, 0.1% SDS, 1.0% Triton X-100, 1.0% sodium deoxycholate) containing protease inhibitors (Halt, Thermo Scientific) and 100 μg samples were electrophoresed on 10% SDS-polyacrylamide gels. After electrophoresis, samples were transferred to nitrocellulose or PVDF membrane, blocked with 5% non-fat milk and immunoblotted using monoclonal mouse anti-TfR1 antibody H68.4 (1:500 or 1:1000, Invitrogen), sheep anti-TfR1 antibody (1:5000, [48]) monoclonal mouse anti-TfR2 antibody 9F81C11 (1:1000, Santa Cruz Biotechnology) or mouse anti-Flag (1:1000, Sigma). As a loading control, blots were probed with mouse anti-actin C4 clone (1:10,000, MP Biomedicals) or mouse anti-tubulin (1:10,000, Sigma). Secondary antibody, IRDye800 or IRDye680 conjugated donkey anti-mouse, donkey anti-rabbit or donkey anti-sheep (1:10,000, LI-COR) was used to detect immunoreactivity using an Odyssey Infrared Imaging System (LI-COR). Relative intensities of protein bands were normalized to actin using Odyssey version 2.1 software.

G647A TfR1 Mutagenesis and Transfection Experiments

The pcDNA3/G647A TfR1 plasmid was generated using QuikChange XL site-directed mutagenesis (Strategene, La Jolla, CA) using a template of pcDNA3/TfR1 and primers of 5'- CTG TAT TCT GCT CGT GCA GAC TTC TTC CGT GC -3' and 5'- GCA CGG AAG AAG TCT GCA CGA GCA GAA TAC AG

-3' following manufacturer's instructions. TRVb cells were transiently transfected to express either wild type TfR1 (2 μg plasmid DNA) or the G647A TfR1 point mutant (2 μg plasmid DNA) using LipofectAMINE2000 (Invitrogen) according to manufacturer's instructions. Cells were split 24 hours post-transfection into 6-well plates and treated with ferristatin II the following day. HeLa cells were transfected with HFE containing a Flag tag (0.5 μg plasmid DNA) or pcDNA vector control (0.5 μg plasmid DNA) as described above.

^{125}I-Transferrin Surface Binding

TRVb cells were grown to 90% confluency in Ham's F-12 medium containing 10% FBS. Cells were transfected as described above with WT TfR1 or G647A TfR1. After 24 hours, cells were plated into 6 well dishes and incubated for an additional 24 hours. Cells were chilled on ice for 15 min and washed twice in ice-cold serum-free Ham's F-12 medium. Cell monolayers were incubated on ice in serum-free Ham's F-12 medium containing 20 mM Hepes, pH 7.4, 2 mg/ml ovalbumin, and 500 nM ^{125}I-Tf with or without 5 μM unlabeled Tf to displace non-specifically bound ligand. After incubation on ice for 2 hours, cells were washed 4 times with PBS^{++} and lysed with solubilization buffer (0.1% Triton X-100, 0.1% NaOH). Cell-associated radioactivity was measured by gamma counting. Data were adjusted to protein levels determined by Bradford assay.

Fluorescence Microscopy

TRVb cells transfected with WT TfR1 or G647A TfR1 were plated onto poly-L-Lysine coated cover slips 24 hours post transfection and incubated for an additional 24 hours at 37°C, 5% CO_2. Cells were washed with PBS^{++} and fixed with 4% paraformaldehyde. Cells were incubated with PBS (non-permeabilized) or PBS +0.1% Triton X-100 (permeabilized), washed with 1% NH_4Cl and blocked with 5% goat serum. The cells were then immunoreacted with mouse anti-human transferrin receptor, OKT9 (eBioscience), followed by goat anti-mouse Alexa 488 (Invitrogen). Cells were imaged using a Zeiss Observer Z1 Axioscope microscope.

RNA Isolation, cDNA Synthesis and Quantitative PCR

Total RNA was isolated using TRIZOL reagent (Invitrogen) according to the manufacturer's instructions. An additional step with Phenol/Chloroform/8-Quinolinol was used to further purify the RNA. Five μg RNA were reverse transcribed using Super-Script lll First-Strand Synthesis System (Invitrogen) using random hexamers and oligo(dt)$_{20}$ primers. Gene expression was analyzed by quantitative real-time PCR using Power SYBR Green PCR Master Mix (Applied Biosystems) on an Applied Biosystems 7300 Real Time PCR System. The cDNA was diluted 1:40 and 6 μl was used as template in a 15 μl reaction volume. The conditions used were: 40 cycles 95°C for 15 s, 55°C for 30 s, and 72°C for 30 s. Analysis was performed in triplicate for each sample. A dissociation curve analysis was performed to detect non-specific products. 36B4 was used as a reference gene. All primers were used at a final concentration of 200 nM. The primers used were: hepcidin 5'-TGACAGTGCGCTGCTGATG-3' (forward), 5'-GGAATTCTTACAGCATTTACAGCAGA-3' (reverse); 36B4 5'-AGATGCAGCAGATCCGCAT-3' (forward) and 5'-GTTCTTGCCCATCAGCACC-3' (reverse). Calculations for relative quantification were done using the comparative C_T method ($\Delta\Delta C_T$).

Urinary Monoacetylbenzidine Determination

Rat urine was centrifuged, reduced with ascorbic acid at 1 mg/ml, acidified to pH ≤3.0 using concentrated HCl and bound to a Strata-X-C SPE column (Phenomenex). After washing, the sample was eluted with 5% ammonium hydroxide in methanol, concentrated in a speedvac and analyzed using HPLC with a Zorbax Eclipse Plus Phenyl-Hexyl column (Agilent Technologies). The mobile phase was a step gradient starting with 95% 10 mM ammonium acetate, pH 4.7 and 5% acetonitrile; reaching 35% ammonium acetate, 65% acetonitrile after 15.5 mins. A flow rate of 1 ml/min and a detection wavelength of 290 nm were used. Fractions corresponding to the monoacetylbenzidine (MAB) elution time were collected from a standard, control and ferristatin ll treated urine samples and further analyzed by LCMS (The Small Molecule Mass Spectrometry Facility at the FAS Center for Systems Biology, Harvard University), confirming the peak corresponded to the molecular mass of MAB.

Other Assays

Urinary creatinine was determined using the Creatinine Reagent Set (Pointe Scientific Inc.) using a modification of the manufacturer's instructions. The working reagent (100 μl) was added to urine samples or a serial dilution of a creatinine standard (5 μl). After incubation at room temperature for 20 mins, the OD was read at 510 nm. These values were used to normalize urinary MAB levels. Serum alanine aminotransferase (ALT) and aspartate aminotransferase (AST) levels were determined using Infinity ALT and AST reagents (Thermo Scientific) according to the manufacturer's instructions. Assays for hematocrit and liver non-heme iron concentrations were performed as previously described [49]. Serum iron levels were determined as described [50].

Results

Ferristatin II Induces Degradation of TfR1

Previous screening of the National Cancer Institute's small molecule Diversity Set library identified ferristatin (NSC30611) as an inhibitor of Tf-mediated iron uptake [43]. Ferristatin's mechanism of action includes down-regulation of TfR1 by a lipid raft pathway that promotes receptor degradation [44]. Subsequent analysis of structural orthologs determined similar properties were associated with a second iron transport inhibitor NSC8679, disodium 4-amino-3-((4′-((2,4-diaminophenyl)azo)-4-biphenyl-l)azo-5-hydroxy-6-(phenylazo)-2,7-naphthalene disulfonate [45]. In this report, we refer to the second compound as ferristatin II. The influence of ferristatin II on Tf-mediated iron uptake was characterized *in vitro* using HeLa cells. Dose-dependent inhibition of cellular ^{55}Fe uptake was observed when cells were treated with up to 100 μM ferristatin II for 4 hours at 37°C in the presence of ^{55}Fe-Tf (Figure 1A). The IC_{50} value of ~ 12 μM was similar to previous results obtained for ferristatin [44]. Western blot analysis confirmed that under these conditions, TfR1 was degraded (Figure 1B). The dose-dependent loss of TfR1 correlates with the reduction in iron uptake activity over this concentration range and provides a molecular explanation for lower cellular ^{55}Fe uptake from Tf due to reduced receptor levels. Degradation of TfR1 was time-dependent with approximately 60–70% of receptors lost within 4 hours of treatment with 50 μM ferristatin II (Figure 1C).

Ferristatin II does not Degrade TfR2 or HFE

TfR1 is known to associate with HFE at the plasma membrane and during endocytosis [51,52]. It is thought that Tf binding to TfR1 promotes dissociation of HFE from TfR1 and promotes its

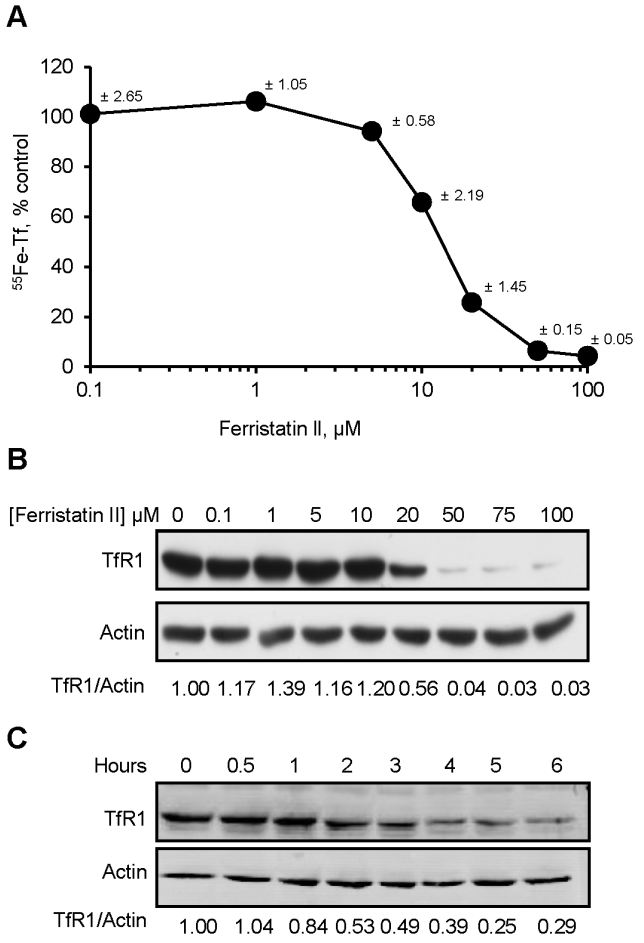

Figure 1. Ferristatin II induces degradation of TfR1 *in vitro*. Panel A: HeLa cells were treated for 4 hours with indicated concentrations of ferristatin II in the presence of 40 nM ^{55}Fe-Tf. Shown are means ± SEM for triplicate values. Panel B: HeLa cell lysates were collected for Western blotting to determine Tf receptor levels. Panel C: Time course studies were carried out with cells treated with 50 μM ferristatin II for up to 6 hours.
doi:10.1371/journal.pone.0070199.g001

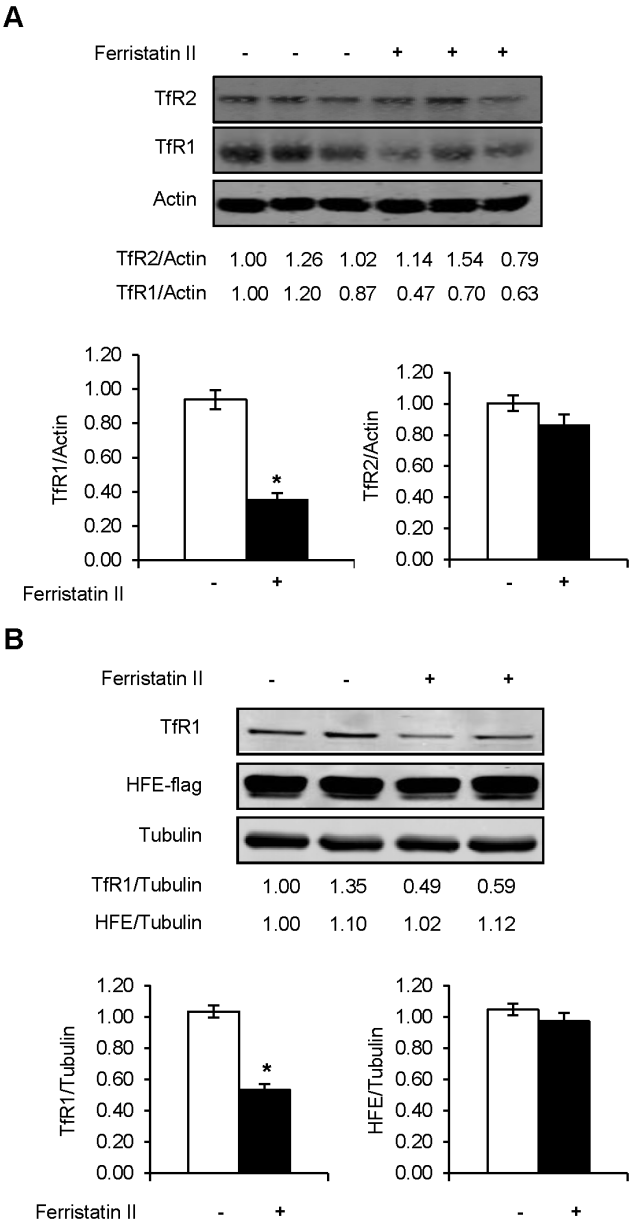

Figure 2. Ferristatin II does not degrade TfR2 or HFE. Panel A: Lysates from Hep3B cells stably expressing TfR2 were collected for Western blotting after 4 hours of 50 μM ferristatin II treatment. Ratios of band density for TfR1/Actin or TfR2/Actin are normalized to vehicle control (DMSO) in the absence of ferristatin II. The bar graph summarizes data from four separate experiments (n = 11 TfR1/Actin $p<0.001$, determined by two-tailed Student's t test, n = 12 TfR2/Actin). Panel B: HeLa cells were transfected to express HFE-flag as described in Materials and Method. Cells were then incubated 4 h with or without 50 μM ferristatin II. Tubulin is shown as a loading control and the indicated values were normalized to control lanes in the absence of ferristatin II. The bar graph represents multiple transfections (n = 8, $p<0.001$ for TfR1/Actin determined by two-tailed Student's t test).
doi:10.1371/journal.pone.0070199.g002

interactions with TfR2, a close homolog of TfR1 [53]. To investigate the specificity of ferristatin II, Hep3B cells stably expressing TfR2 were treated with ferristatin II for 4 hours. Although endogenous TfR1 was degraded, levels of TfR2 were not decreased. (Figure 2A). It has been previously shown that exogenous expression of epitope-tagged HFE can be used to monitor its interaction with TfR1 [51,52]. Therefore HeLa cells were transfected to transiently express flag-tagged HFE, then treated with ferristatin II. Levels of flag-tagged HFE were unaffected by ferristatin II while TfR1 was still degraded (Figure 2B). These results show that ferristatin II selectively induces the loss of TfR1.

Ferristatin II Induced Degradation of TfR1 is Sensitive to Bafilomycin and Nystatin

It has been previously shown that ferristatin-induced TfR1 degradation is blocked by lysosomal inhibitors [44]. In a similar fashion, bafilomycin A_1, which raises the pH in intracellular compartments, also blocks TfR1 degradation induced by ferristatin (Figure 3A). These findings are consistent with the idea that receptors are internalized for degradation. Past studies with ferristatin also have shown that endocytosis through lipid

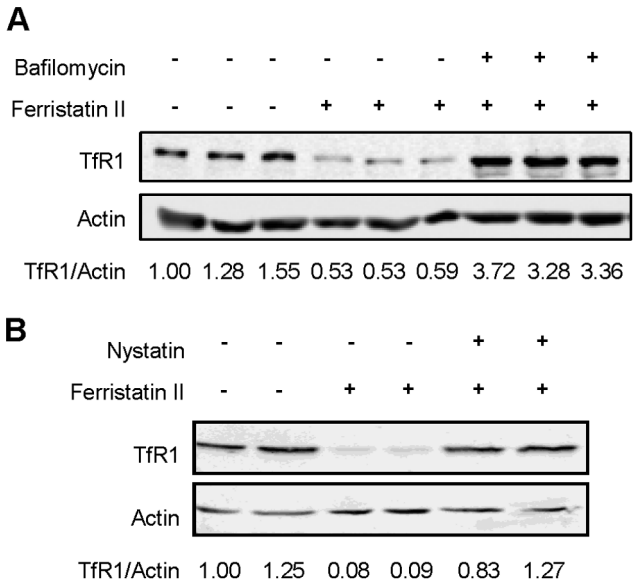

Figure 3. Ferristatin II induced degradation is bafilomycin and nystatin sensitive. Panel A: HeLa cells were treated overnight with 10 nM bafilomycin A_1 prior to 4 h treatment with or without 50 μM ferristatin II in the presence of 10 nM bafilomycin A_1. Blot is representative of several experiments. Panel B: HeLa cells were pre-treated for 30 minutes with 25 μg/mL nystatin or left untreated. After incubation, cells were treated with 50 μM ferristatin II for 4 hours. Shown below are the density ratios for TfR1/Actin normalized to control lanes (DMSO treated) in the absence of ferristatin II. Shown is a representative blot from several similar experiments.
doi:10.1371/journal.pone.0070199.g003

raft domains was necessary for TfR1 degradation [44]. To explore the possible role of lipid rafts in ferristatin II's mechanism of action, we used the cholesterol binding agent nystatin to disrupt lipid rafts [54,55]. The effects of ferristatin II on TfR1 degradation were antagonized by the presence of nystatin (Figure 3B).

TfR1 Domains Necessary for Clathrin Pathway Interactions are not Necessary for Ferristatin II Induced Degradation

Two "internalization defective" TfR1 mutants were studied. Y20C/F23A TfR1 harbors point mutations within the receptor's endocytic motif, while Δ3–28 TfR1 is a deletion mutant lacking 25 amino acids of the domain [21]. This domain is responsible for interaction with AP-2 and the clathrin machinery. Previous investigations by McGraw and coworkers established stable expression of these mutants in TRVb cells, which lack endogenous Tf receptors [46]. Effects of ferristatin II on TRVb cells expressing the Y20C/F23A or Δ3–28 TfR1 mutants were compared to TRVb1 cells expressing wild-type TfR1 as a control (Figure 4A). Both receptor mutants were degraded upon ferristatin II treatment, although the time course of degradation was delayed compared to wild-type TfR1 (Figure 4B).

Tf Blocks Ferristatin II Action

Since it is known that clathrin-mediated endocytosis of TfR1 occurs regardless of receptor occupancy [56,57,58], we examined the effects of Tf on TfR1 degradation by ferristatin II. In the presence of holo-Tf, the action of ferristatin II to induce degradation of TfR1 was blocked (Figure 5). There are at least two possible explanations for the observed antagonism: ferristatin II competes with holo-Tf for binding to TfR1 or Tf acts as a non-specific antagonist of ferristatin II action. Therefore, a receptor point mutant, G647A TfR1, was constructed to probe the receptor's ligand-binding domain. Gly647 resides in the RGD sequence previously shown to be critical for Tf binding [59,60]. The ability of ferristatin II to degrade wild type and G647A TfR1 was tested in TRVb cells. Transiently expressed G647A TfR1 was distributed in these cells in a fashion similar to wild type as shown by immunofluorescence microscopy (Figure 6A). As predicted, the mutant receptor failed to bind ^{125}I-labeled Tf (Figure 6B). Cells transiently transfected to express either wild-type receptor or the G647A mutant were treated with or without 50 μM ferristatin II in the presence or absence of holo-Tf. Western blot analysis confirmed that holo-Tf blocked ferristatin II induced degradation of wild-type TfR1 but it did not interfere with G647A TfR1 degradation (Figure 6C). Therefore, binding of ligand to the receptor blocks ferristatin II action.

Effects of Ferristatin II *in vivo*

To examine whether effects of ferristatin II observed *in vitro* reflect its activity *in vivo*, rats were injected twice daily with vehicle, 0.2, 10 and 40 mg/kg of the drug for one or three days, then once in the morning of the second or fourth day prior to tissue collection. Monoacetylbenzidine, a known metabolite [61], was detected in urine after 4 days of treatment at higher doses. Serum ALT and AST activities were measured to assess possible liver damage; serum ALT was slightly elevated at the highest dose but AST was not significantly affected (Figure 7). These results demonstrate the drug is metabolized by acetylation with minimal toxicity over the time course and doses administered in our experiments.

Significant changes in liver non-heme iron levels were not observed over the course of ferristatin II treatment (Figure 7). However, Tf saturation and serum iron levels were reduced after 2 days of treatment and significantly lower at all concentrations tested for the 4 day treatments. Western blot analysis revealed TfR1 levels were significantly reduced in livers from treated rats compared to vehicle-injected controls, consistent with the action of ferristatin II to degrade receptors *in vitro* (Figure 8A). It has been proposed that dissociation of HFE from TfR1 promotes synthesis of the iron regulatory hormone hepcidin [31,32]. Hepcidin then acts on the iron exporter ferroportin to reduce systemic iron levels. qPCR analysis revealed that hepcidin synthesis was enhanced in rats treated with ferristatin II with ~ 9-fold increase in mRNA levels relative to control (vehicle-injected) rats (Figure 8B). Reduced intestinal iron absorption was also observed in rats treated with ferristatin II in uptake experiments that determined the amount of ^{59}Fe in blood after intragastric gavage (Figure 8C).

Discussion

It has been long established that TfR1 enters cells through clathrin-mediated endocytosis [6]. This pathway is particularly well understood in the context of cellular iron delivery [62]. However, under some circumstances cell surface proteins like epidermal growth factor receptor (EGFR) [63], the glucose transporter GLUT4 [64] and TGF-β family members [65] are internalized via lipid rafts in addition to clathrin dependent mechanisms. Early observations with the first iron transport inhibitor, ferristatin, indicated that like these other membrane proteins, TfR1 could undergo lipid raft mediated internalization [44]. Ferristatin induced degradation of TfR1 was sensitive to

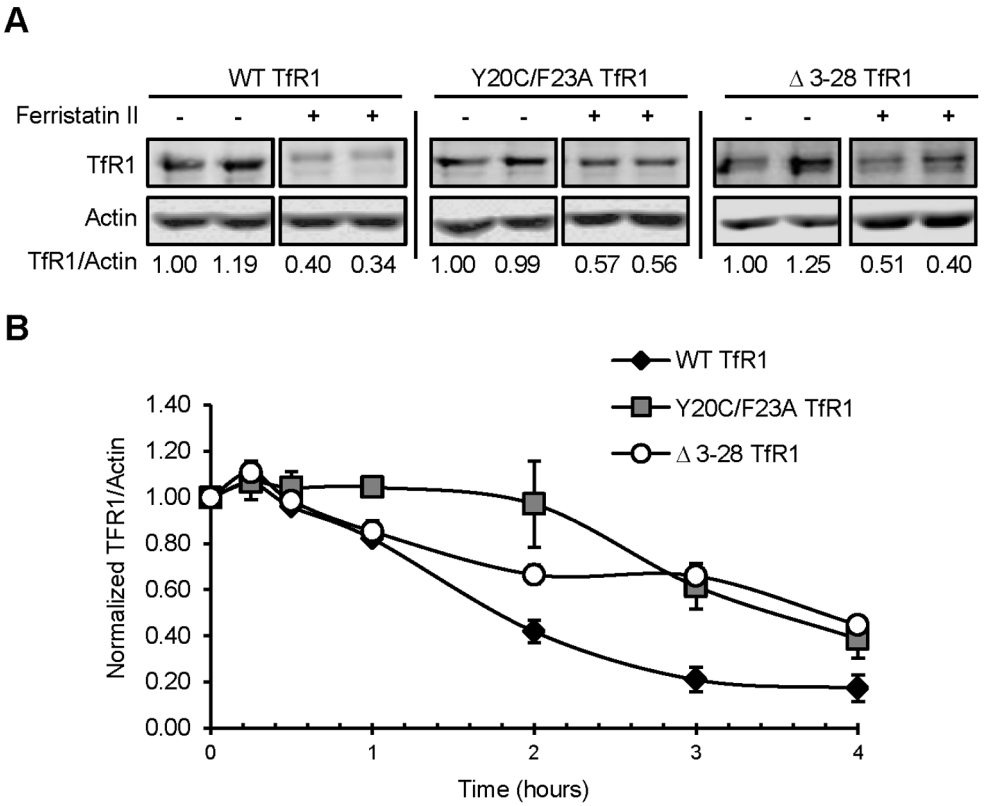

Figure 4. Ferristatin induced degradation is independent of an interaction with the clathrin endocytic machinery. Panel A: TRVb cells stably transfected to express WT TfR1, Y20C/F23A TfR1, or Δ3–28 TfR1 were treated for 4 hours with 50 μM ferristatin II. Density ratios for TfR1/Actin normalized to control lanes (DMSO treated) in the absence of ferristatin II are indicated for each lane. Nonconsecutive lanes are separated by a white space. Individual blots are separated by a black bar. All blots were probed using a sheep-TfR1 antibody raised against the ectodomain of TfR1. Panel B: Time course of WT TfR1, Y20C/F23A TfR1 and Δ3–28 TfR1 degradation after 0–4 hour incubation with 50 μM ferristatin II. Shown are mean TfR1/Actin ratios ± SEM from 3 separate experiments performed in duplicate.
doi:10.1371/journal.pone.0070199.g004

filipin and nystatin, two cholesterol-depleting drugs that implicate a role for lipid rafts. Although nystatin-sensitivity has been noted in some examples of clathrin-mediated endocytosis [66], knock-down of clathrin did not interfere with TfR1 degradation induced by ferristatin [44], further supporting the function of the lipid raft pathway in the drug's action. Our characterization of ferristatin II activity reveals that this second member of the ferristatin family of iron transport inhibitors induces degradation of TfR1 both *in vivo* and *in vitro*. The loss of receptors explains why cells in culture treated with ferristatin II have lower ^{55}Fe uptake from Tf. Our results further confirm sensitivity of the degradation pathway to nystatin. Our studies of TRVb1 cells stably expressing various receptor mutants defective in clathrin-mediated endocytosis [21] suggest that elements of the TfR1 cytoplasmic domain necessary for clathrin-mediated endocytosis may not be required for ferristatin II-induced degradation. These independent lines of evidence indicate that ferristatin II mediates degradation of TfR1 by a non-clathrin pathway, and a role for lipid rafts is suggested by the sensitivity to cholesterol depletion.

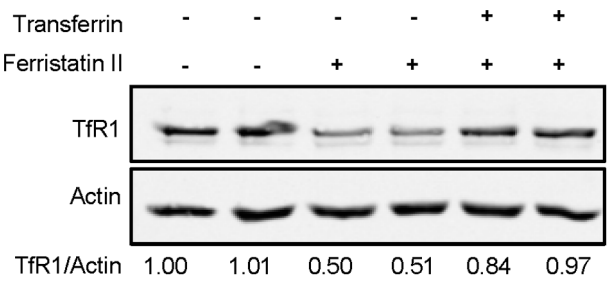

Figure 5. Tf blocks ferristatin II induced receptor degradation. HeLa cells were treated for 4 hours with 50 μM ferristatin II with or without 1 mg/mL Tf. Shown below are the density ratios for TfR1/Actin normalized to control lanes (DMSO treated) in the absence of ferristatin II. Shown is a representative blot with similar results observed on several separate occasions.
doi:10.1371/journal.pone.0070199.g005

The importance of lipid rafts in iron metabolism and signaling is just beginning to be elucidated. For example, degradation of the iron exporter ferroportin induced by the iron regulatory hormone hepcidin is disrupted by cholesterol depletion [67] and ferroportin has been shown to fractionate in detergent-resistant membrane fractions with flotillin or caveolin-1, both markers of lipid rafts [67]. Finally, the cholesterol binding protein CD133 is known to influence Tf uptake in Caco-2 cells [68]. Such evidence suggests a prominent role for lipid rafts in the regulation of iron metabolism. Regulation of the lipid raft pathway by iron status provides an additional layer in the complex regulation of iron transport. The ability to pharmacologically induce an alternative TfR1 membrane trafficking mechanism through lipid rafts provides an

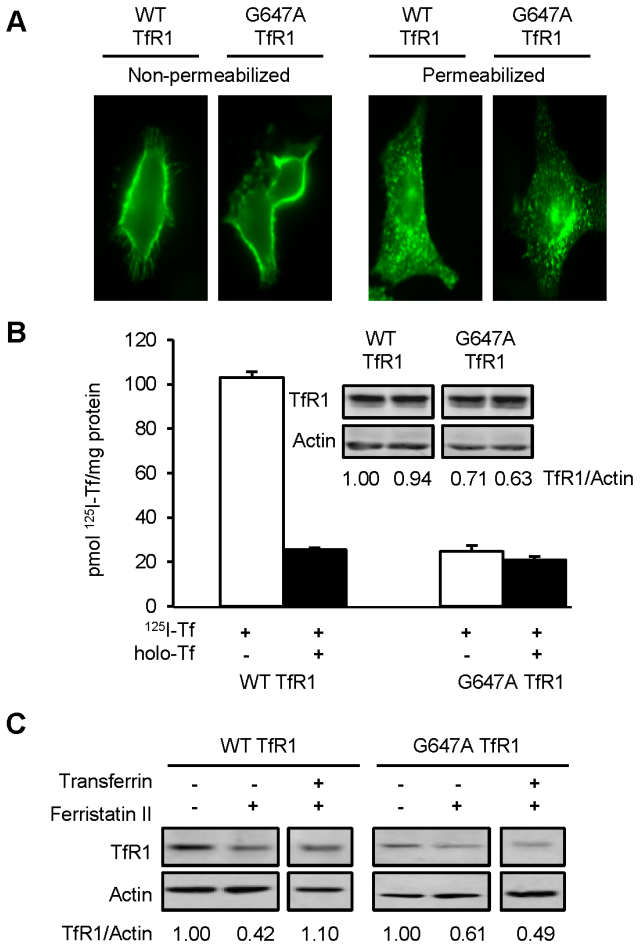

Figure 6. Ferristatin II induces degradation of ligand binding mutant G647A TfR1. Panel A: TRVb cells were transfected with 1 μg WT TfR1 or G647A TfR1, plated on poly-L-lysine coated cover slips and fixed with 4% paraformaldehyde. Cells were immunoreacted with OKT9 (α-TfR1) followed by goat anti-mouse Alexa 488 and imaged using a Zeiss Observer Z1 Axioscope microscope. Panel B: TRVb cells were transfected as in (A) in 6-well plates and incubated for 48 hours (see Experimental Procedures for details). Cells were then chilled, washed and incubated with 500 nM ^{125}I-Tf in the absence or presence of 5 μM unlabeled Tf for 2 hours. After washing and lysis, cell associated radioactivity was measured by γ-counting. Absolute deviation for duplicate values for cells with 500 nM ^{125}I-Tf (open bars) or 500 nM ^{125}I-Tf +5 μM Tf (closed bars) is shown. Inset: Western blot confirms equivalent expression levels for WT and G647A TfR1. Panel C: TRVb cells, transfected with WT or G647A TfR1 were treated for 4 hours with 50 μM ferristatin II with or without 1 mg/mL Tf. Shown below are the density ratios for TfR1/Actin normalized to control lanes (DMSO treated) in the absence of ferristatin II. Nonconsecutive lanes are separated by a white space. Blot is representative of several experiments (n = 6, WT and G647A TfR1).
doi:10.1371/journal.pone.0070199.g006

interesting new avenue to modulate the delivery of iron with potential clinical application.

Unlike clathrin-mediated TfR1 endocytosis, which occurs independent of receptor occupancy, the presence of Tf antagonizes ferristatin II-induced degradation. The finding that G647A TfR1 with defective ligand binding is susceptible to ferristatin II suggests that Tf may occlude the drug's interactions with wild-type TfR1. Alternatively, Tf interactions with the receptor could induce conformational changes that block ferristatin II binding to a distal domain, possibly including the cytoplasmic domain. Further work is necessary to more precisely define structural elements of TfR1 that contribute to targeting by ferristatin II. Our results indicate these effects are quite specific since ferristatin II does not affect protein levels of TfR2 expressed in Hep3B cells. Although structurally related, TfR1 and TfR2 differ in domain interactions with both HFE and Tf [47]. Sensitivity to degradation by ferristatin II marks another structural distinction between the two receptors that should be further explored.

The ability of ferristatin II to reduce TfR1 levels *in vivo* was confirmed by administering the drug to rats at doses up to 40 mg/kg. Serum iron and transferrin saturation were lowered after 2 days of treatment, and significantly reduced at all concentrations of ferristatin II tested after 4 days of treatment. These effects were associated with a ~50% decrease in the protein level of TfR1 in liver. Notably, hepatic non-heme iron content did not change. The lack of change in hepatic iron despite hypoferremia is consistent with a block in iron mobilization. Our intragastric gavage experiments show that rats treated with ferristatin II also have reduced intestinal uptake of ^{59}Fe to the blood. Both of these observations can be explained by the observed up-regulation of hepcidin, a regulatory hormone of iron metabolism [38]. Hepcidin interacts with the iron exporter ferroportin to induce its lysosomal degradation, thereby blocking dietary absorption [35] and release of iron stores [69]. Hepcidin is known to be induced by increasing Tf saturation under high iron conditions which triggers dissociation of HFE from TfR1 [31] coupled to its association with stabilized TfR2 [32]. Since ferristatin II degrades TfR1 but not HFE, we hypothesize the action of ferristatin II releases HFE to promote hepcidin synthesis. In this scenario, receptor degradation rather than high iron promotes HFE association with TfR2, and possibly activates other factors that regulate hepcidin expression [70,71]. As shown in Figure 9, under basal conditions, HFE is bound to TfR1. As levels of iron saturated Tf increase, Tf outcompetes HFE for binding to TfR1. Released HFE can bind TfR2 to initiate a signaling cascade promoting hepcidin synthesis. In the presence of ferristatin II, the degradation of TfR1 liberates HFE to bind TfR2 and induce hepcidin synthesis in the liver. This action appears to be independent of high iron, since rats treated with ferristatin II display hypoferremia yet continue to upregulate hepcidin synthesis.

It is important to consider that other targets of ferristatin II action may contribute to the effects we observe. *In vitro* studies have shown that ferristatin II also inhibits transport of iron by DMT1 [45], and this transporter plays an important role in apical iron uptake by enterocytes [72,73]. Inhibition of DMT1 activity would reduce iron absorption, leading to lower serum iron and transferrin saturation independent of hepcidin's action on ferroportin. On the other hand, some reports have suggested that hepcidin also regulates DMT1 function in the intestine [74], so that direct suppression of DMT1 might also arise due to hepcidin induction by ferristatin II. Regardless of the precise target(s), inhibition of import and/or export of iron across the intestinal mucosa provides a rational explanation for the reduced level of circulating iron observed in rats treated with ferristatin II. The idea that increased hepcidin blocks iron mobilization from stores, a known action of the hormone (67), is also consistent with the observation that non-heme iron levels in liver are not altered by ferristatin II treatment.

Several other pharmacological tools now have been developed to target the hepcidin axis [75], including "mini-hepcidins" that down-regulate ferroportin [76,77], BMP inhibitors that block Smad signaling [78,79], and agents that perturb Stat signaling

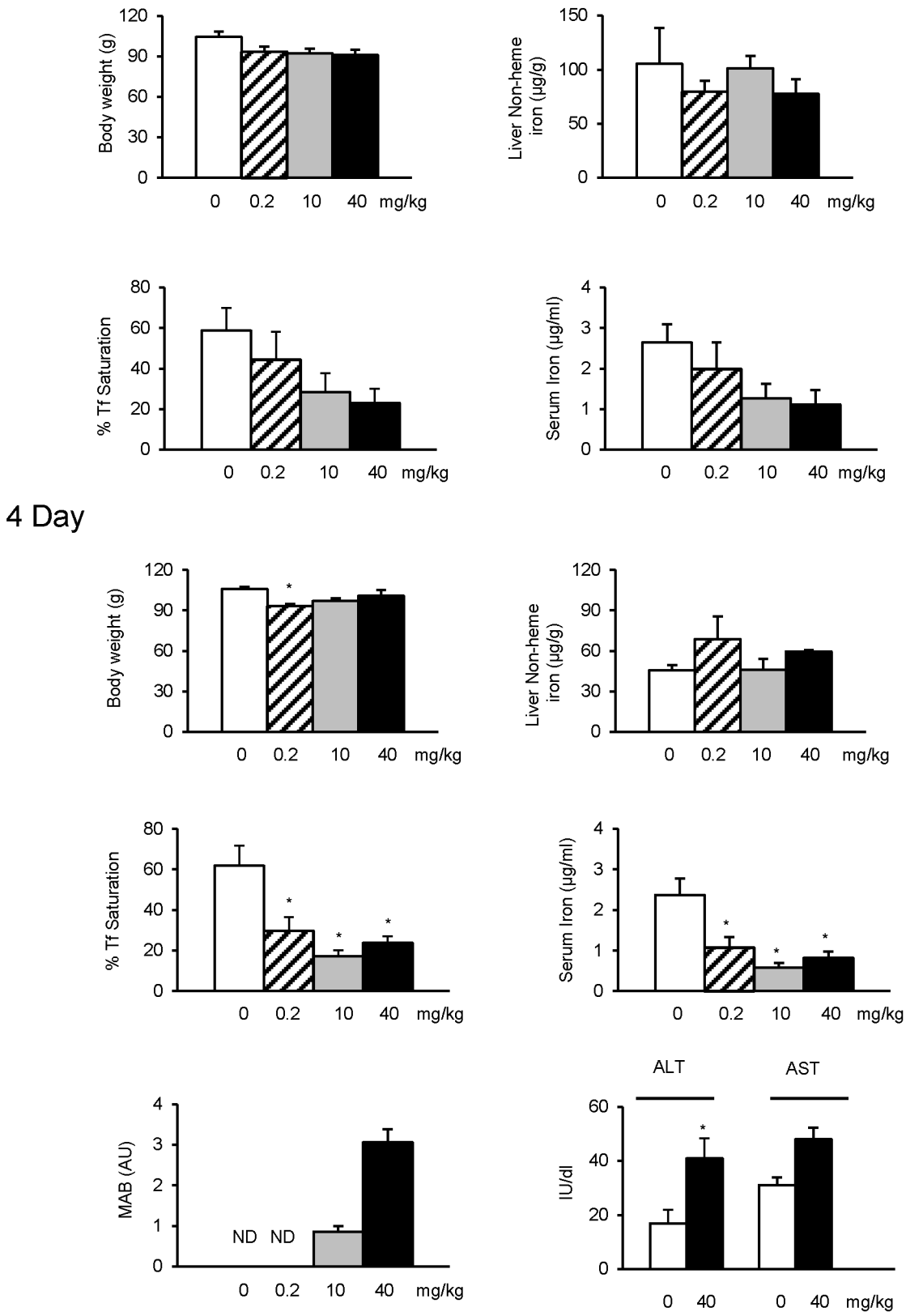

Figure 7. Effects of ferristatin II *in vivo*. Rats were treated with vehicle control (saline) or 0.2, 10 or 40 mg/kg ferristatin II for 2 or 4 days as described in Experimental Procedures. Shown are mean values ± SEM (n = 4) for body weight (*P = 0.022), liver non-heme iron, Tf saturation (*P = 0.018, 0.002 and 0.006 for 0.2, 10 and 40 mg/kg, respectively) and serum iron levels (*P = 0.016, 0.002 and 0.005 for 0.2, 10 and 40 mg/kg,

respectively) measured after a 6 h fasting period. P values were determined by one-way ANOVA followed by Tukey's test as a post hoc comparison. Monoacetylbenzidine (MAB) levels in rat urine were determined by HPLC and normalized to creatinine levels (arbitrary units). Shown are means ± SEM (AU = arbitrary units; ND = not detected. Serum ALT and AST activities were determined using ALT and AST reagents (Thermo Scientific) for rats injected for 4 days with vehicle or 40 mg/kg ferristatin II. Shown are means ± SEM (n = 3–6; *P = 0.033 determined by two-tailed Student's t test).
doi:10.1371/journal.pone.0070199.g007

[80,81]. The ferristatins are unique in targeting TfR1 degradation [43,44]. We previously have shown that degradation of the receptor induced by ferristatin occurs through a lipid raft-dependent mechanism [44]. Recently, the antimalarial agent dihydroartemisinin was shown to degrade TfR1 [82]. Depletion of cellular iron through this mechanism was proposed to account for this drug's anticancer effects. Interestingly, down-regulation of TfR1 by dihydroartemisinin also was shown to proceed via a lipid raft mechanism. The alternative TfR1 membrane trafficking mechanism revealed by use of small molecule inhibitors provides an intriguing new pathway to potentially regulate iron metabolism in a number of different disease states.

Acknowledgments

We thank Dorathy Vargas for technical assistance with animal care and injections.

Author Contributions

Conceived and designed the experiments: SLB JK MWR. Performed the experiments: SLB PB JK FL JS. Analyzed the data: SLB PB JK FL JS. Contributed reagents/materials/analysis tools: JC CE. Wrote the paper: SLB PB MWR.

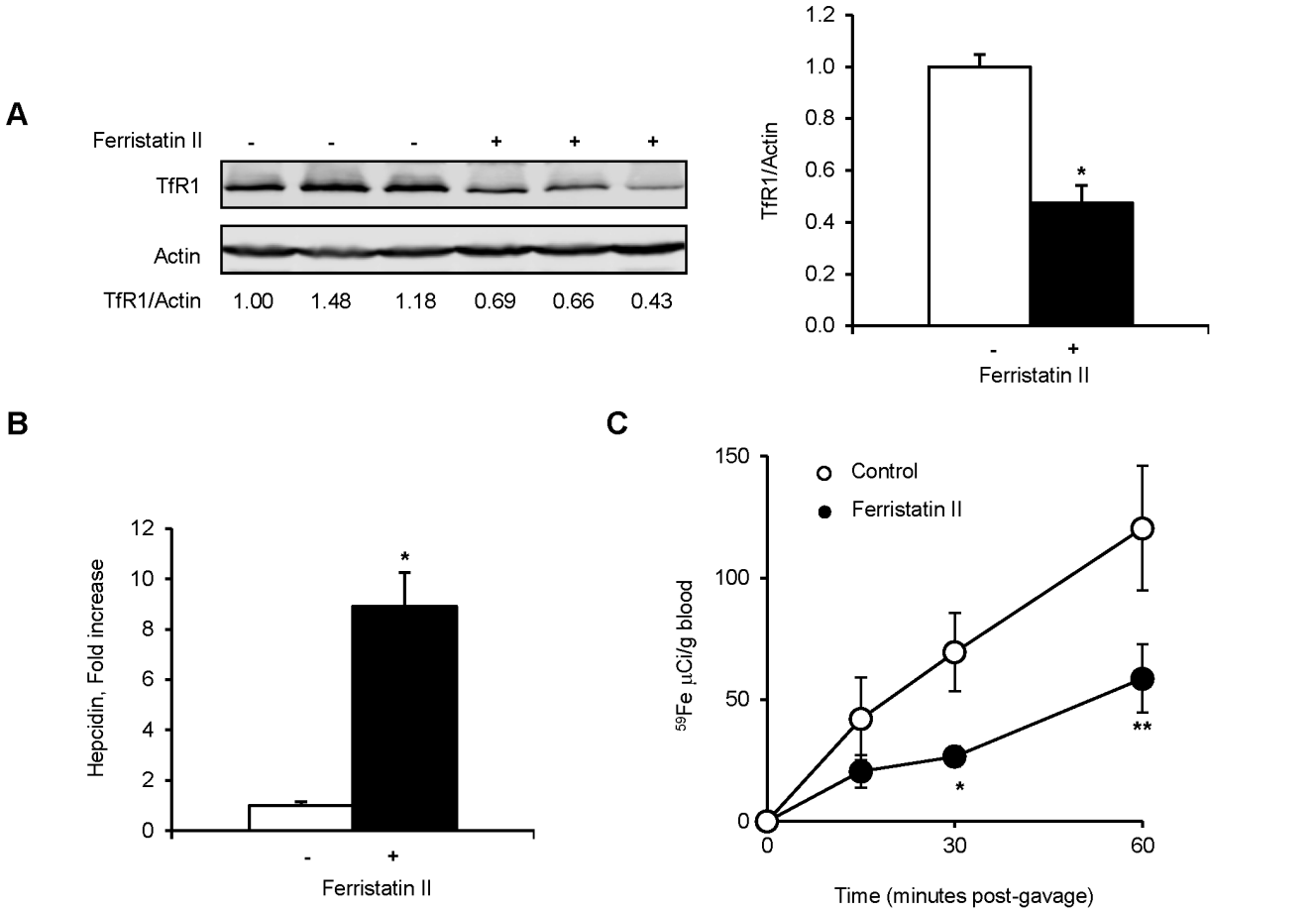

Figure 8. Ferristatin II alters iron homeostasis *in vivo*. Panel A: Liver lysates from rats injected with saline or 40 mg/kg ferristatin II for 4 days were immunoblotted to determine TfR1 levels. Actin was used as a loading control. Bar graph shows normalized TfR1/actin ratio as the mean ± SEM (n = 7; *P<0.001 determined by two-tailed Student's t test). Panel B: Liver RNA was isolated, reverse transcribed and qPCR performed as described under Experimental Procedures. Data were normalized to levels of 36B4. Shown are means ± SEM (n = 5–7; *P<0.001 determined by two-tailed Student's t test). Panel C: To determine intestinal iron absorption, control and treated rats were fasted for 4 h and ^{59}Fe was administered by gavage. Blood samples were drawn at indicated times and radioactivity was determined by gamma counting. Shown are means ± SEM for control (open circles; n = 4–6) and ferristatin II (closed circles; n = 7–8; *P = 0.01 and **P = 0.05 determined by two-tailed Student's t test).
doi:10.1371/journal.pone.0070199.g008

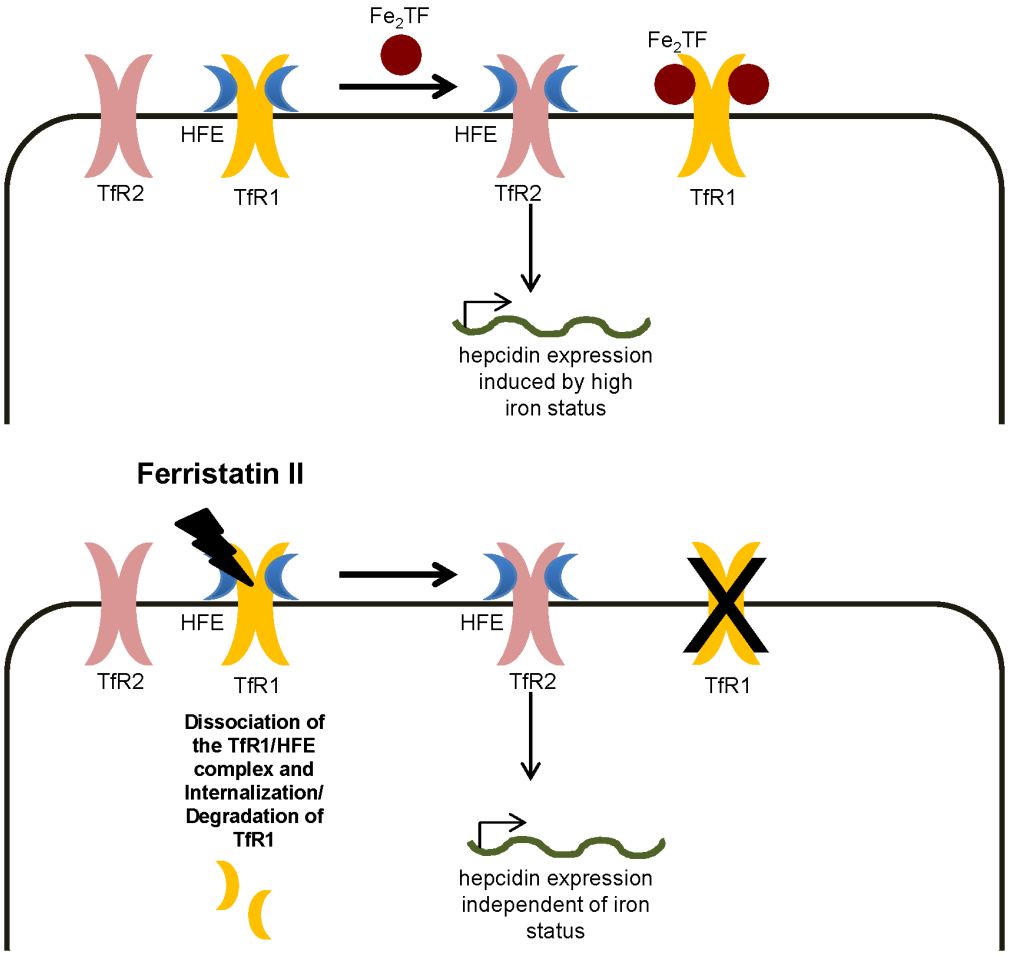

Figure 9. Model of iron homeostasis under normal and ferristatin II conditions. The contributors to iron metabolism include TfR1, TfR2, Tf and HFE. These molecules work together to maintain systemic iron homeostasis by sensing high and low iron levels. See text for details.
doi:10.1371/journal.pone.0070199.g009

References

1. Aisen P, Listowsky I (1980) Iron transport and storage proteins. Annu Rev Biochem 49: 357–393.
2. Lederman HM, Cohen A, Lee JW, Freedman MH, Gelfand EW (1984) Deferoxamine: a reversible S-phase inhibitor of human lymphocyte proliferation. Blood 64: 748–753.
3. Seligman PA, Schleicher RB, Siriwardana G, Domenico J, Gelfand EW (1993) Effects of agents that inhibit cellular iron incorporation on bladder cancer cell proliferation. Blood 82: 1608–1617.
4. Noulsri E, Richardson DR, Lerdwana S, Fucharoen S, Yamagishi T, et al. (2009) Antitumor activity and mechanism of action of the iron chelator, Dp44mT, against leukemic cells. Am J Hematol 84: 170–176.
5. Ciechanover A, Schwartz AL, Lodish HF (1983) The asialoglycoprotein receptor internalizes and recycles independently of the transferrin and insulin receptors. Cell 32: 267–275.
6. van Renswoude J, Bridges KR, Harford JB, Klausner RD (1982) Receptor-mediated endocytosis of transferrin and the uptake of Fe in K562 cells: identification of a nonlysosomal acidic compartment. Proc Natl Acad Sci U S A 79: 6186–6190.
7. Ohgami RS, Campagna DR, Greer EL, Antiochos B, McDonald A, et al. (2005) Identification of a ferrireductase required for efficient transferrin-dependent iron uptake in erythroid cells. Nat Genet 37: 1264–1269.
8. Lambe T, Simpson RJ, Dawson S, Bouriez-Jones T, Crockford TL, et al. (2009) Identification of a Steap3 endosomal targeting motif essential for normal iron metabolism. Blood 113: 1805–1808.
9. Fleming MD, Romano MA, Su MA, Garrick LM, Garrick MD, et al. (1998) Nramp2 is mutated in the anemic Belgrade (b) rat: evidence of a role for Nramp2 in endosomal iron transport. Proc Natl Acad Sci U S A 95: 1148–1153.
10. Zhao N, Gao J, Enns CA, Knutson MD (2010) ZRT/IRT-like protein 14 (ZIP14) promotes the cellular assimilation of iron from transferrin. J Biol Chem 285: 32141–32150.
11. Dong XP, Cheng X, Mills E, Delling M, Wang F, et al. (2008) The type IV mucolipidosis-associated protein TRPML1 is an endolysosomal iron release channel. Nature 455: 992–996.
12. Dautry-Varsat A, Ciechanover A, Lodish HF (1983) pH and the recycling of transferrin during receptor-mediated endocytosis. Proc Natl Acad Sci U S A 80: 2258–2262.
13. Klausner RD, Van Renswoude J, Ashwell G, Kempf C, Schechter AN, et al. (1983) Receptor-mediated endocytosis of transferrin in K562 cells. J Biol Chem 258: 4715–4724.
14. Herbison CE, Thorstensen K, Chua AC, Graham RM, Leedman P, et al. (2009) The role of transferrin receptor 1 and 2 in transferrin-bound iron uptake in human hepatoma cells. Am J Physiol Cell Physiol 297: C1567–1575.
15. Ciechanover A, Schwartz AL, Dautry-Varsat A, Lodish HF (1983) Kinetics of internalization and recycling of transferrin and the transferrin receptor in a human hepatoma cell line. Effect of lysosomotropic agents. J Biol Chem 258: 9681–9689.
16. Beardmore J, Howell KE, Miller K, Hopkins CR (1987) Isolation of an endocytic compartment from A431 cells using a density modification procedure employing a receptor-specific monoclonal antibody complexed with colloidal gold. J Cell Sci 87 (Pt 4): 495–506.
17. Zuk PA, Elferink LA (2000) Rab15 differentially regulates early endocytic trafficking. J Biol Chem 275: 26754–26764.
18. McMahon HT, Boucrot E (2011) Molecular mechanism and physiological functions of clathrin-mediated endocytosis. Nat Rev Mol Cell Biol 12: 517–533.
19. McGraw TE, Maxfield FR (1990) Human transferrin receptor internalization is partially dependent upon an aromatic amino acid on the cytoplasmic domain. Cell Regul 1: 369–377.
20. Ohno H, Stewart J, Fournier MC, Bosshart H, Rhee I, et al. (1995) Interaction of tyrosine-based sorting signals with clathrin-associated proteins. Science 269: 1872–1875.

21. Pytowski B, Judge TW, McGraw TE (1995) An internalization motif is created in the cytoplasmic domain of the transferrin receptor by substitution of a tyrosine at the first position of a predicted tight turn. J Biol Chem 270: 9067–9073.
22. Hinshaw JE, Schmid SL (1995) Dynamin self-assembles into rings suggesting a mechanism for coated vesicle budding. Nature 374: 190–192.
23. Sweitzer SM, Hinshaw JE (1998) Dynamin undergoes a GTP-dependent conformational change causing vesiculation. Cell 93: 1021–1029.
24. Babitt JL, Huang FW, Wrighting DM, Xia Y, Sidis Y, et al. (2006) Bone morphogenetic protein signaling by hemojuvelin regulates hepcidin expression. Nat Genet 38: 531–539.
25. Feder JN, Gnirke A, Thomas W, Tsuchihashi Z, Ruddy DA, et al. (1996) A novel MHC class I-like gene is mutated in patients with hereditary haemochromatosis. Nat Genet 13: 399–408.
26. Camaschella C, Roetto A, Cali A, De Gobbi M, Garozzo G, et al. (2000) The gene TFR2 is mutated in a new type of haemochromatosis mapping to 7q22. Nat Genet 25: 14–15.
27. Montosi G, Donovan A, Totaro A, Garuti C, Pignatti E, et al. (2001) Autosomal-dominant hemochromatosis is associated with a mutation in the ferroportin (SLC11A3) gene. J Clin Invest 108: 619–623.
28. Roetto A, Papanikolaou G, Politou M, Alberti F, Girelli D, et al. (2003) Mutant antimicrobial peptide hepcidin is associated with severe juvenile hemochromatosis. Nat Genet 33: 21–22.
29. Papanikolaou G, Samuels ME, Ludwig EH, MacDonald ML, Franchini PL, et al. (2004) Mutations in HFE2 cause iron overload in chromosome 1q-linked juvenile hemochromatosis. Nat Genet 36: 77–82.
30. Gao J, Chen J, De Domenico I, Koeller DM, Harding CO, et al. (2010) Hepatocyte-targeted HFE and TFR2 control hepcidin expression in mice. Blood 115: 3374–3381.
31. Schmidt PJ, Toran PT, Giannetti AM, Bjorkman PJ, Andrews NC (2008) The transferrin receptor modulates Hfe-dependent regulation of hepcidin expression. Cell Metab 7: 205–214.
32. Gao J, Chen J, Kramer M, Tsukamoto H, Zhang AS, et al. (2009) Interaction of the hereditary hemochromatosis protein HFE with transferrin receptor 2 is required for transferrin-induced hepcidin expression. Cell Metab 9: 217–227.
33. Schmidt PJ, Andrews NC, Fleming MD (2010) Hepcidin induction by transgenic overexpression of Hfe does not require the Hfe cytoplasmic tail, but does require hemojuvelin. Blood 116: 5679–5687.
34. Vujic Spasic M, Kiss J, Herrmann T, Galy B, Martinache S, et al. (2008) Hfe acts in hepatocytes to prevent hemochromatosis. Cell Metab 7: 173–178.
35. Nemeth E, Tuttle MS, Powelson J, Vaughn MB, Donovan A, et al. (2004) Hepcidin regulates cellular iron efflux by binding to ferroportin and inducing its internalization. Science 306: 2090–2093.
36. Canonne-Hergaux F, Donovan A, Delaby C, Wang HJ, Gros P (2006) Comparative studies of duodenal and macrophage ferroportin proteins. Am J Physiol Gastrointest Liver Physiol 290: G156–163.
37. Donovan A, Lima CA, Pinkus JL, Pinkus GS, Zon LI, et al. (2005) The iron exporter ferroportin/Slc40a1 is essential for iron homeostasis. Cell Metab 1: 191–200.
38. Pigeon C, Ilyin G, Courselaud B, Leroyer P, Turlin B, et al. (2001) A new mouse liver-specific gene, encoding a protein homologous to human antimicrobial peptide hepcidin, is overexpressed during iron overload. J Biol Chem 276: 7811–7819.
39. Weinstein DA, Roy CN, Fleming MD, Loda MF, Wolfsdorf JI, et al. (2002) Inappropriate expression of hepcidin is associated with iron refractory anemia: implications for the anemia of chronic disease. Blood 100: 3776–3781.
40. Bridle KR, Frazer DM, Wilkins SJ, Dixon JL, Purdie DM, et al. (2003) Disrupted hepcidin regulation in HFE-associated haemochromatosis and the liver as a regulator of body iron homoeostasis. Lancet 361: 669–673.
41. Nemeth E, Roetto A, Garozzo G, Ganz T, Camaschella C (2005) Hepcidin is decreased in TFR2 hemochromatosis. Blood 105: 1803–1806.
42. Byrne SL, Krishnamurthy D, Wessling-Resnick M (2013) Pharmacology of iron transport. Annu Rev Pharmacol Toxicol 53: 17–36.
43. Brown JX, Buckett PD, Wessling-Resnick M (2004) Identification of small molecule inhibitors that distinguish between non-transferrin bound iron uptake and transferrin-mediated iron transport. Chem Biol 11: 407–416.
44. Horonchik L, Wessling-Resnick M (2008) The small-molecule iron transport inhibitor ferristatin/NSC306711 promotes degradation of the transferrin receptor. Chem Biol 15: 647–653.
45. Buckett PD, Wessling-Resnick M (2009) Small molecule inhibitors of divalent metal transporter-1. Am J Physiol Gastrointest Liver Physiol 296: G798–804.
46. McGraw TE, Greenfield L, Maxfield FR (1987) Functional expression of the human transferrin receptor cDNA in Chinese hamster ovary cells deficient in endogenous transferrin receptor. J Cell Biol 105: 207–214.
47. Chen J, Chloupkova M, Gao J, Chapman-Arvedson TL, Enns CA (2007) HFE modulates transferrin receptor 2 levels in hepatoma cells via interactions that differ from transferrin receptor 1-HFE interactions. J Biol Chem 282: 36862–36870.
48. Warren RA, Green FA, Enns CA (1997) Saturation of the endocytic pathway for the transferrin receptor does not affect the endocytosis of the epidermal growth factor receptor. J Biol Chem 272: 2116–2121.
49. Heilig E, Molina R, Donaghey T, Brain JD, Wessling-Resnick M (2005) Pharmacokinetics of pulmonary manganese absorption: evidence for increased susceptibility to manganese loading in iron-deficient rats. Am J Physiol Lung Cell Mol Physiol 288: L887–893.
50. Kim J, Molina RM, Donaghey TC, Buckett PD, Brain JD, et al. (2011) Influence of DMT1 and iron status on inflammatory responses in the lung. Am J Physiol Lung Cell Mol Physiol 300: L659–665.
51. Feder JN, Penny DM, Irrinki A, Lee VK, Lebron JA, et al. (1998) The hemochromatosis gene product complexes with the transferrin receptor and lowers its affinity for ligand binding. Proc Natl Acad Sci U S A 95: 1472–1477.
52. Gross CN, Irrinki A, Feder JN, Enns CA (1998) Co-trafficking of HFE, a nonclassical major histocompatibility complex class I protein, with the transferrin receptor implies a role in intracellular iron regulation. J Biol Chem 273: 22068–22074.
53. Goswami T, Andrews NC (2006) Hereditary hemochromatosis protein, HFE, interaction with transferrin receptor 2 suggests a molecular mechanism for mammalian iron sensing. J Biol Chem 281: 28494–28498.
54. Parton RG, Richards AA (2003) Lipid rafts and caveolae as portals for endocytosis: new insights and common mechanisms. Traffic 4: 724–738.
55. Brown DA (2006) Lipid rafts, detergent-resistant membranes, and raft targeting signals. Physiology (Bethesda) 21: 430–439.
56. Watts C (1985) Rapid endocytosis of the transferrin receptor in the absence of bound transferrin. J Cell Biol 100: 633–637.
57. Stein BS, Sussman HH (1986) Demonstration of two distinct transferrin receptor recycling pathways and transferrin-independent receptor internalization in K562 cells. J Biol Chem 261: 10319–10331.
58. Girones N, Davis RJ (1989) Comparison of the kinetics of cycling of the transferrin receptor in the presence or absence of bound diferric transferrin. Biochem J 264: 35–46.
59. Dubljevic V, Sali A, Goding JW (1999) A conserved RGD (Arg-Gly-Asp) motif in the transferrin receptor is required for binding to transferrin. Biochem J 341 (Pt 1): 11–14.
60. West AP, Giannetti AM, Herr AB, Bennett MJ, Nangiana JS, et al. (2001) Mutational analysis of the transferrin receptor reveals overlapping HFE and transferrin binding sites. J Mol Biol 313: 385–397.
61. Bos RP, Groenen MA, Theuws JL, Leijdekkers CM, Henderson PT (1984) Metabolism of benzidine-based dyes and the appearance of mutagenic metabolites in urine of rats after oral or intraperitoneal administration. Toxicology 31: 271–282.
62. Richardson DR, Ponka P (1997) The molecular mechanisms of the metabolism and transport of iron in normal and neoplastic cells. Biochim Biophys Acta 1331: 1–40.
63. Sigismund S, Woelk T, Puri C, Maspero E, Tacchetti C, et al. (2005) Clathrin-independent endocytosis of ubiquitinated cargos. Proc Natl Acad Sci U S A 102: 2760–2765.
64. Blot V, McGraw TE (2006) GLUT4 is internalized by a cholesterol-dependent nystatin-sensitive mechanism inhibited by insulin. Embo J 25: 5648–5658.
65. Di Guglielmo GM, Le Roy C, Goodfellow AF, Wrana JL (2003) Distinct endocytic pathways regulate TGF-beta receptor signalling and turnover. Nat Cell Biol 5: 410–421.
66. Subtil A, Gaidarov I, Kobylarz K, Lampson MA, Keen JH, et al. (1999) Acute cholesterol depletion inhibits clathrin-coated pit budding. Proc Natl Acad Sci U S A 96: 6775–6780.
67. Auriac A, Willemetz A, Canonne-Hergaux F (2010) Lipid raft-dependent endocytosis: a new route for hepcidin-mediated regulation of ferroportin in macrophages. Haematologica 95: 1269–1277.
68. Bourseau-Guilmain E, Griveau A, Benoit JP, Garcion E (2011) The importance of the stem cell marker prominin-1/CD133 in the uptake of transferrin and in iron metabolism in human colon cancer Caco-2 cells. PLoS One 6: e25515.
69. Ganz T (2007) Molecular control of iron transport. J Am Soc Nephrol 18: 394–400.
70. Finberg KE, Heeney MM, Campagna DR, Aydinok Y, Pearson HA, et al. (2008) Mutations in TMPRSS6 cause iron-refractory iron deficiency anemia (IRIDA). Nat Genet 40: 569–571.
71. Du X, She E, Gelbart T, Truksa J, Lee P, et al. (2008) The serine protease TMPRSS6 is required to sense iron deficiency. Science 320: 1088–1092.
72. Fleming MD, Trenor CC 3rd, Su MA, Foernzler D, Beier DR, et al. (1997) Microcytic anaemia mice have a mutation in Nramp2, a candidate iron transporter gene. Nat Genet 16: 383–386.
73. Gunshin H, Mackenzie B, Berger UV, Gunshin Y, Romero MF, et al. (1997) Cloning and characterization of a mammalian proton-coupled metal-ion transporter. Nature 388: 482–488.
74. Brasse-Lagnel C, Karim Z, Letteron P, Bekri S, Bado A, et al. (2011) Intestinal DMT1 cotransporter is down-regulated by hepcidin via proteasome internalization and degradation. Gastroenterology 140: 1261–1271 e1261.
75. Sun CC, Vaja V, Babitt JL, Lin HY (2012) Targeting the hepcidin-ferroportin axis to develop new treatment strategies for anemia of chronic disease and anemia of inflammation. Am J Hematol 87: 392–400.
76. Preza GC, Ruchala P, Pinon R, Ramos E, Qiao B, et al. (2011) Minihepcidins are rationally designed small peptides that mimic hepcidin activity in mice and may be useful for the treatment of iron overload. J Clin Invest 121: 4880–4888.
77. Ramos E, Ruchala P, Goodnough JB, Kautz L, Preza GC, et al. (2012) Minihepcidins prevent iron overload in a hepcidin-deficient mouse model of severe hemochromatosis. Blood 120: 3829–3836.
78. Theurl I, Schroll A, Sonnweber T, Nairz M, Theurl M, et al. (2011) Pharmacologic inhibition of hepcidin expression reverses anemia of chronic inflammation in rats. Blood 118: 4977–4984.

79. Babitt JL, Huang FW, Xia Y, Sidis Y, Andrews NC, et al. (2007) Modulation of bone morphogenetic protein signaling in vivo regulates systemic iron balance. J Clin Invest 117: 1933–1939.
80. Song SN, Tomosugi N, Kawabata H, Ishikawa T, Nishikawa T, et al. (2010) Down-regulation of hepcidin resulting from long-term treatment with an anti-IL-6 receptor antibody (tocilizumab) improves anemia of inflammation in multicentric Castleman disease. Blood 116: 3627–3634.
81. Fatih N, Camberlein E, Island ML, Corlu A, Abgueguen E, et al. (2010) Natural and synthetic STAT3 inhibitors reduce hepcidin expression in differentiated mouse hepatocytes expressing the active phosphorylated STAT3 form. J Mol Med (Berl) 88: 477–486.
82. Ba Q, Zhou N, Duan J, Chen T, Hao M, et al. (2012) Dihydroartemisinin exerts its anticancer activity through depleting cellular iron via transferrin receptor-1. PLoS One 7: e42703.